

## The Role of $T_{50}$ in the Classification of Gamma-ray Bursts\*

Xiao-Hong Zhao, Yi-Ping Qin, Yun-Ming Dong and Zhao-Yang Peng

Yunnan Observatory, Chinese Academy of Sciences, Kunming 650011;  
agns00@public.km.yn.cn

Received 2003 October 24; accepted 2004 January 12

**Abstract** The role of  $T_{50}$  in classifying gamma-ray bursts (GRBs) is investigated. We take  $T_{50} = 0.7$  s as the line of division and find that some bursts belonging to the class of long bursts defined by  $T_{90} \geq 2$  s now become short bursts (sample 1), while some belonging to the class of short bursts defined by  $T_{90} < 2$  s now become long bursts (sample 2). We study how these sources are affected by the two methods of classification and find the change of classes of sample 1 is due to some peculiar properties of the light curves. Based on their characters, most of the bursts of sample 1 should be taken as short bursts.

**Key words:** gamma ray: bursts — gamma ray: observations

### 1 INTRODUCTION

Gamma-ray bursts (GRBs) have been discovered for about 30 years (Klebesadel et al. 1973). As more and more data, especially those of BATSE, are obtained, many properties of GRBs have been revealed, but some still remain unclear. With so much available data (e.g., Fishman et al. 1994; Meegan 1994; Meegan et al. 1996, 1998; Paciesas et al. 1999), quite a number of statistical analyses have been carried out. Possible correlations among various parameters were analyzed (see, e.g., Golenetskii et al. 1983; Barat et al. 1984; Belli 1993; Malozzi et al. 1995; Dezalay et al. 1997; Belli 1999; Qin et al. 2000). Kouveliotou et al. (1993) divided the GRBs into two classes of long and short bursts using the  $T_{90}$  distribution of 222 bursts from the first BATSE catalog. With the BATSE data Fishman (1999) confirmed the correlation between the hardness ratio and the duration ( $T_{90}$ ). Qin et al. (2000) found that the hardness ratio and the duration were only correlated for the entire set of the 4B catalog, while they were not at all correlated for either of the two classes of GRBs, thus confirming the existence of two classes of GRBs.

While  $T_{90}$  certainly plays an important role in classifying GRBs, in the following we will investigate the classification according to  $T_{50}$ .

### 2 CHANGE OF THE BURSTS IN THE TWO CLASSIFICATIONS

The GRBs were divided into two classes of long and short durations at  $T_{90} = 2$  s (e.g., Dezalay et al. 1992; Kouveliotou et al. 1993; Fishman et al. 1994; Meegan et al. 1996; Pa-

---

\* Supported by the National Natural Science Foundation of China.

ciasas et al. 1999). Kouveliotou et al. (1993) constructed the distribution of  $T_{50}$  for the first BATSE catalog, and found the bimodality is not so significant. However, Paciesas et al. (1999) constructed the same distribution for the data of 4B (bursts between 1991 April 19 and 1996 August 29) and found the bimodality to be quite evident.

In the current BATSE Catalog (spanning from 1991 to 2000) there are 1956 bursts with values of both  $T_{50}$  and  $T_{90}$  and values of fluence in both channels 2 and 3. With this new set of data, we can construct a new  $T_{50}$  distribution.

First, following previous work, we calculate the hardness ratio HR defined as the fluence in channel 3 ( $\sim 100$  to  $\sim 300$  keV) divided by the fluence in channel 2 ( $\sim 50$  to  $\sim 100$ ), and obtain the  $\log \text{HR} - \log T_{50}$  plot shown in Fig. 1. For comparison we also show the plot of  $\log \text{HR}$  versus  $\log T_{90}$  (Fig. 2). In both plots, one can see there are two prominent clusters.

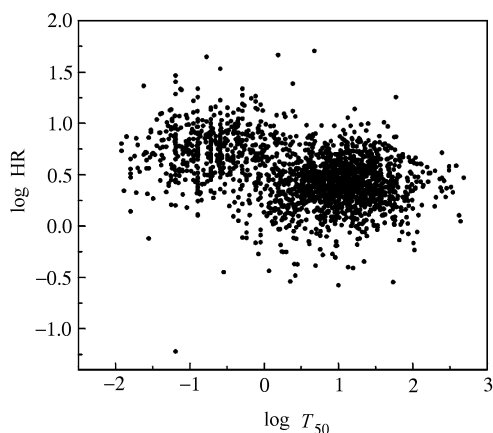


Fig. 1 Plot of  $\log \text{HR} - \log T_{50}$  for all the bursts.  $T_{50}$  is in units of second.

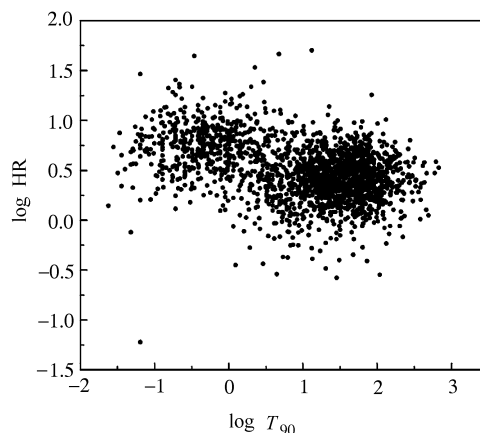


Fig. 2 Plot of  $\log \text{HR} - \log T_{90}$  for all the bursts.  $T_{90}$  is in units of second.

Secondly, we plot the distribution of  $T_{50}$  for all the burst; this is shown in Fig. 3. It is evident there are two peaks and between the peaks there is a dip located at about 0.7 s. We divide the bursts into two subsets at 0.7 s: 461 short-duration bursts with  $T_{50} < 0.7$  s and 1495 long-duration bursts with  $T_{50} > 0.7$  s. If we use the previous criterion of  $T_{90}=2$  s we will have 1488 long bursts and 468 short bursts.

There are 27 bursts (sample 1) with  $T_{90} \geq 2$  s and  $T_{50} < 0.7$  s, and 34 bursts (sample 2) with  $T_{90} < 2$  s and  $T_{50} \geq 0.7$  s. To find a proper value of  $T_{50}$  in dividing the bursts into two subclasses in an independent way, a correlation analysis of  $T_{90}$  and  $T_{50}$  for all the bursts is made (see Fig. 4). The correlation coefficient between  $\log T_{90}$  and  $\log T_{50}$  is  $r = 0.968$ , showing that the correlation is definitely significant. Now that the correlation of the two quantities is confirmed, we can read off the value of  $T_{50}$  corresponding to the value of  $T_{90} = 2$  s on the regression line, and we obtain  $T_{50} = 0.753$  s. With this value we redivide the bursts into two classes and find that 28 previous long bursts ( $T_{90} \geq 2$  s) now become short bursts ( $T_{50} < 0.753$  s) and 28 previous short bursts ( $T_{90} < 2$  s) now become long bursts ( $T_{50} \geq 0.753$  s). Since the number of the sources changing from one class to the other is almost the same in the two ways and since 0.753 s is quite close to 0.7 s, we infer that 0.7 s is suitable for dividing the bursts into two subclasses.

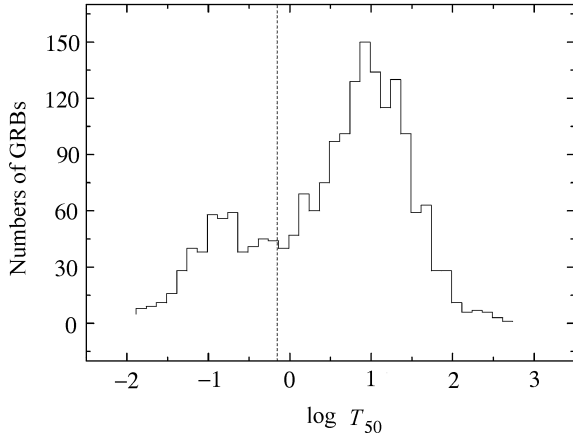


Fig. 3 Distribution of  $T_{50}$  for all the bursts. Dashed line marks the dividing point of 0.7 s.

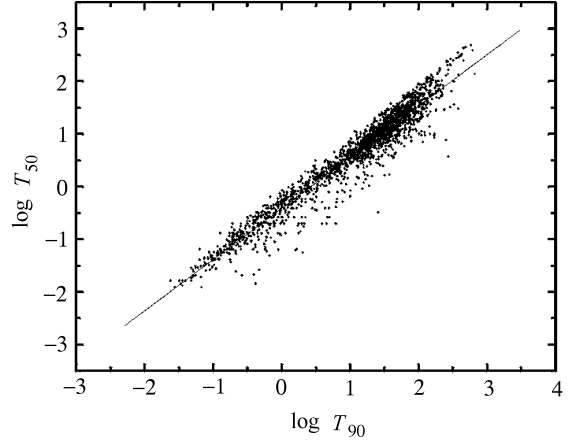


Fig. 4 Plot of  $\log T_{50} - \log T_{90}$  for all the bursts.  $T_{90}$  is in units of second. The solid line is the line of regression.

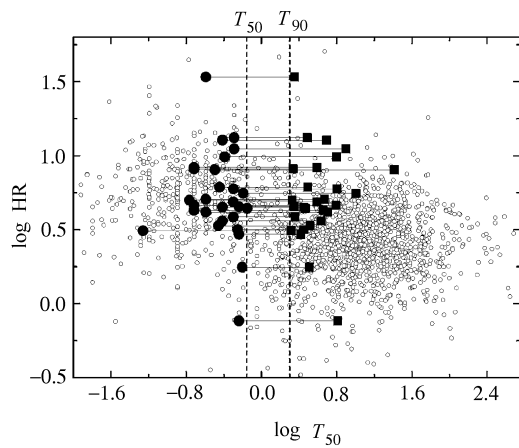


Fig. 5 Plot of  $\log HR - \log T_{50}$ . The open circles are the data plotted in Fig.1. The sample 1 objects are marked with filled circles, while their  $T_{90}$ -values are marked with filled squares. The right dashed line stands for  $T_{90} = 2$  s, and the left dashed line,  $T_{50} = 0.7$  s. Solid lines connect the  $T_{50}$  and  $T_{90}$ -values of sample 1 sources.

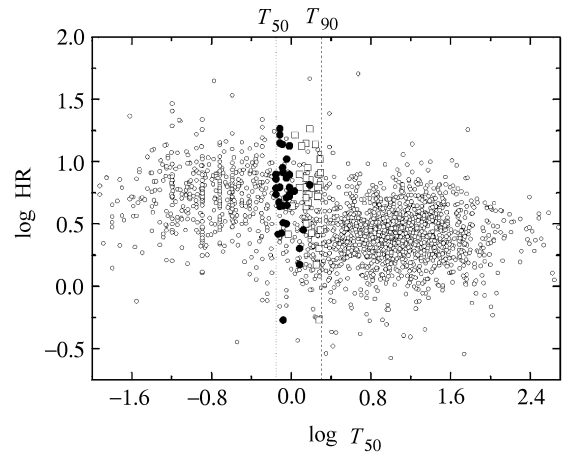


Fig. 6 Plot of  $\log HR - \log T_{50}$ . The open circles are the data points plotted in Fig.1. Sample 2 sources are marked with filled circles, while their  $T_{90}$ -values are marked with filled squares. The two dashed lines have the same meaning as in Fig. 5.

To obtain an intuitive view of how the sources of samples 1 and 2 change from one previous class to the other, we made Figs. 5 and 6. The values of  $T_{50}$  and  $T_{90}$  for the sources of sample 1 are highlighted by large symbols in Fig. 5, where we find that the changes of the values are quite significant. In Fig. 6, the values of  $T_{90}$  and  $T_{50}$  for the sources of sample 2 are highlighted, and we find the changes are not so significant. We suspect that the large changes in sample 1 may result from some peculiar features in their light curves, while the small changes in sample 2 may come from a certain “boundary effect”.

### 3 CHARACTERS OF LIGHT CURVES OF SAMPLE 1

It is noticeable that the change of  $T_{90}$  and  $T_{50}$  in sample 1 is so great. We try to examine the cause leading to the change through analyzing the light curve. To check the characters of the sources of sample 1, we plot their light curves (the data of three sources in sample 1 are absent) in Fig. 7, where the start and end points of  $T_{50}$  and  $T_{90}$  for each source are lined out. From the figure we find for some sources (20 events) signals obviously above the noise last a short time. Among these sources, the light curves of the bursts of 3814, 5439, 5711, 6096, 6281, 6436, 6641, 7305, 7430, 7456, 7599, and 7671 take on a complex structure, where a multimodality can be observed, while those of the bursts of 6182, 6205, 6206, 6238, 6292, 7187, 7290, and 7775 show a simpler structure, where a single peak can be seen. The interval of  $T_{90}$  of these sources covers a sufficient interval of the background. However, for other sources (1953, 2988, 7455 and 8082), signals obviously above the noise last a long time, and the interval of  $T_{90}$  covers only signals, with very short interval of background being included.

In addition, we find for all the sources of the sample the interval of  $T_{50}$  is within the dominant component of the signal well. Weaker components have a great effect on the positions of the starting and ending points of  $T_{90}$ . Since the interval of  $T_{90}$  would include almost all the components, the interval covering all the components (strong or weak) would decide the length of  $T_{90}$ .

### 4 DISCUSSION AND CONCLUSIONS

In the above sections, we analyze the plot of  $\log \text{HR} - \log T_{50}$  of 1956 GRBs and study the duration distribution of  $T_{50}$ . We divide all the bursts into two classes according to the distribution of  $T_{50}$  and find that except 61 sources the classification based on  $T_{50}$  is consistent with that based on  $T_{90}$ . There are 27 bursts (sample 1) with  $T_{90} \geq 2$  s and  $T_{50} < 0.7$  s, and 34 bursts (sample 2) with  $T_{90} < 2$  s and  $T_{50} \geq 0.7$  s. Light curves of the sources of sample 1 are drawn to show how the changes happen.

We know that  $T_{90}$  measures the duration of the time interval during which 90% of the total observed counts have been detected. The start of the  $T_{90}$  interval is defined by the time at which 5% of the total counts have been detected, and the end of the  $T_{90}$  interval is defined by the time at which 95% of the total counts have been detected.  $T_{50}$  is similarly defined using the times at which 25% and 75% of the counts have been detected (4B Duration Table Description 27 Nov, 2001 BATSE GRB Team, <http://www.batse.msfc.nasa.gov>). For the sources of 3814, 5439, 5711, 6096, 6182, 6205, 6206, 6238, 6281, 6292, 6436, 6641, 7187, 7290, 7305, 7430, 7456, 7599, 7671, and 7775, their signals last shortly (case 1), while for 1953, 2988, 7455, and 8082, their signals cover a sufficient interval of time (case 2). For case 1, we suspect that the counts of background are not sufficiently subtracted and therefore lead to the change of the sources (to be short or long bursts) in the two classifications. In fact, it is the remaining background counts that make the value of  $T_{90}$  much longer than it should be. However, it has no or much less effect on the value of  $T_{50}$ . We believe that if the counts of background are sufficiently subtracted,  $T_{90}$  of these sources will become much shorter and these bursts will turn to be short ones. Therefore, it would be better to classify these sources to be short bursts.

In case 2,  $T_{90}$  is mainly contributed by signals. Because of the long interval of signals of these bursts, their  $T_{90}$  is large. Nevertheless,  $T_{50}$  of these bursts is short as it is determined mainly by the dominant signal. For these bursts, different signals have different contributions to the total count. The dominant signal contributes most of the count, while other signals

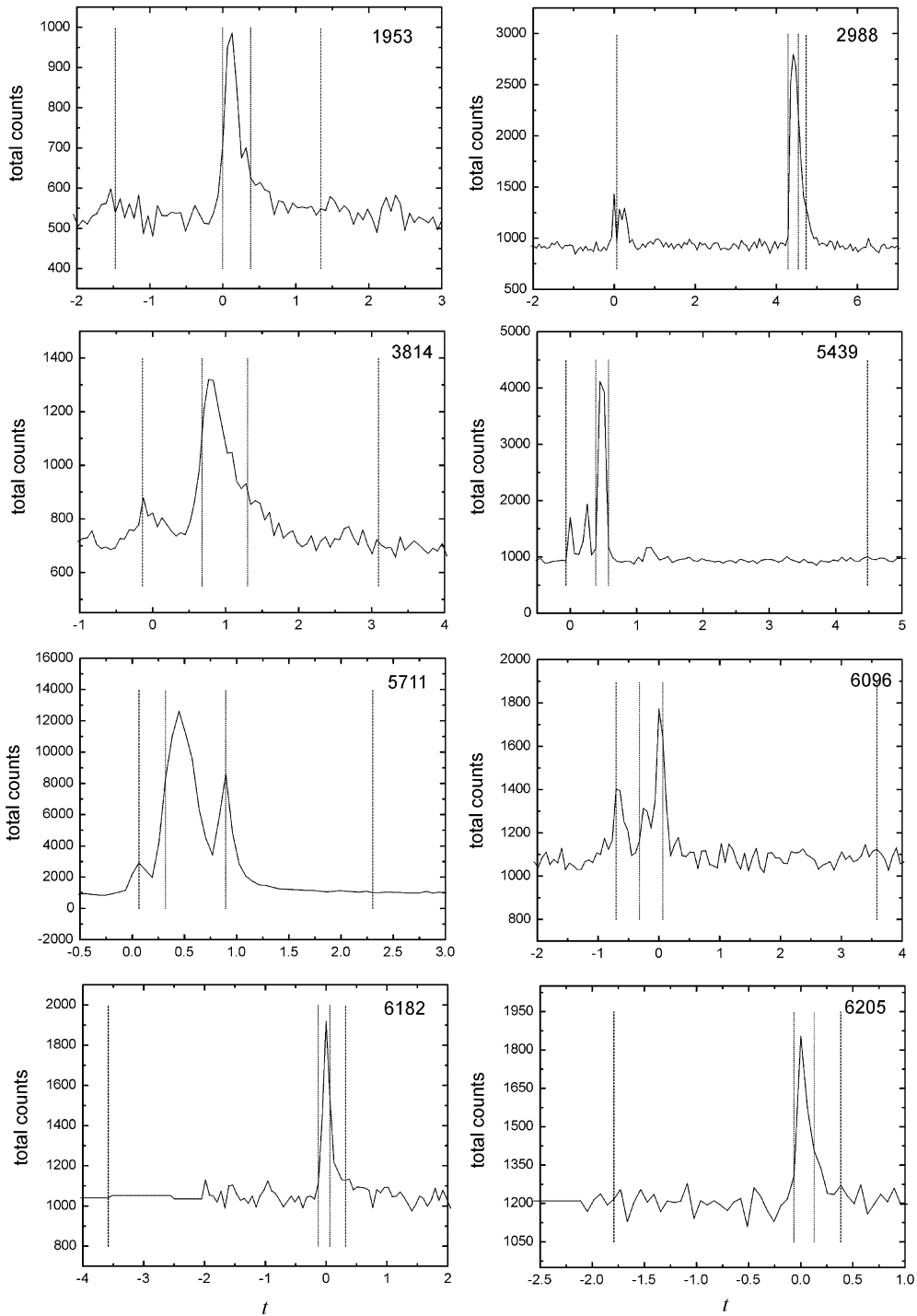


Fig. 7 Light curves of sample 1,  $t$  is in units of second. Total counts are the sum of four energy channels. The two dashed lines are the start and end point of  $T_{90}$ , respectively, while the two dotted lines are the start and the end point of  $T_{50}$ , respectively. The number on the top-right corner of every picture is the trigger number.

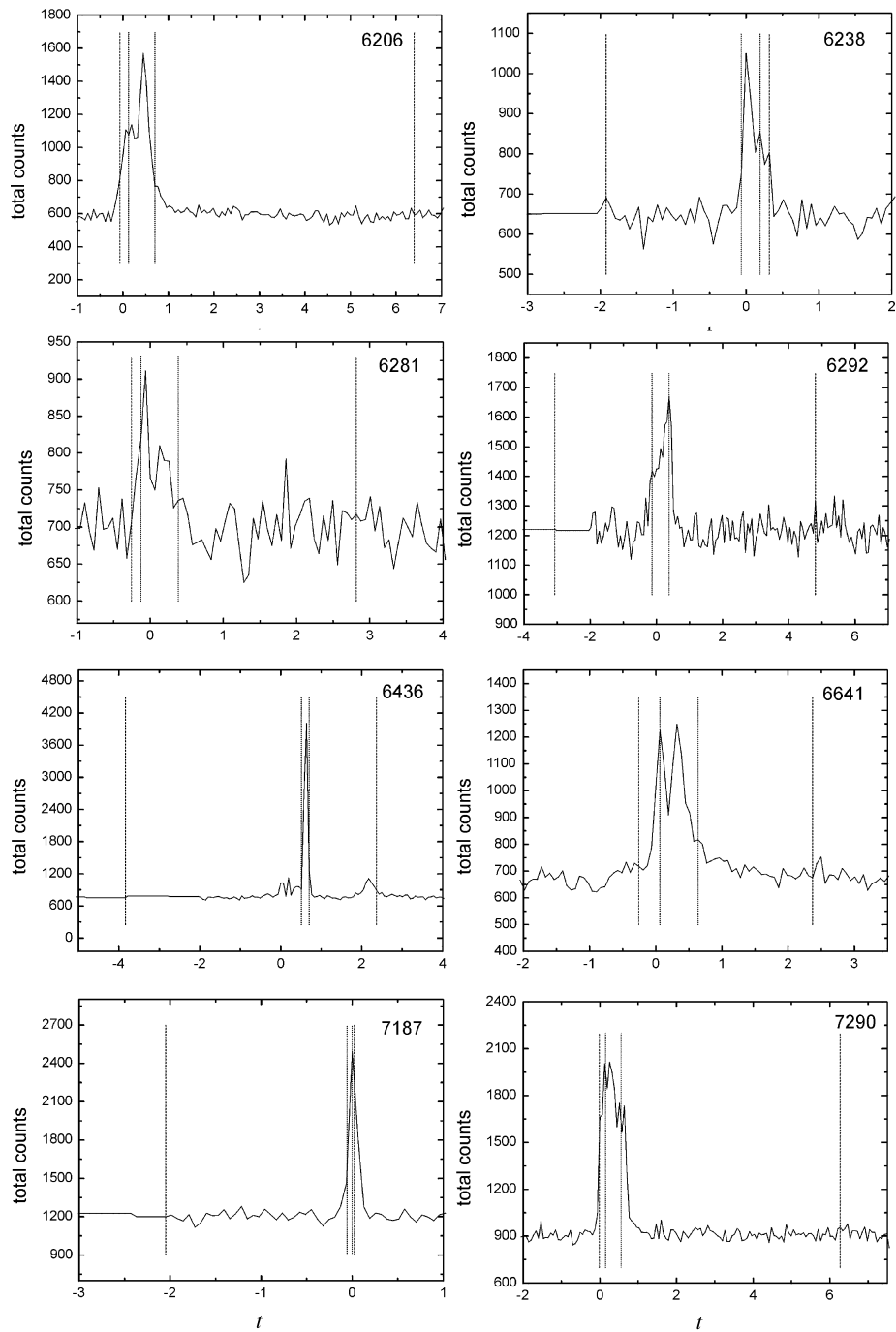


Fig. 7 Continued.

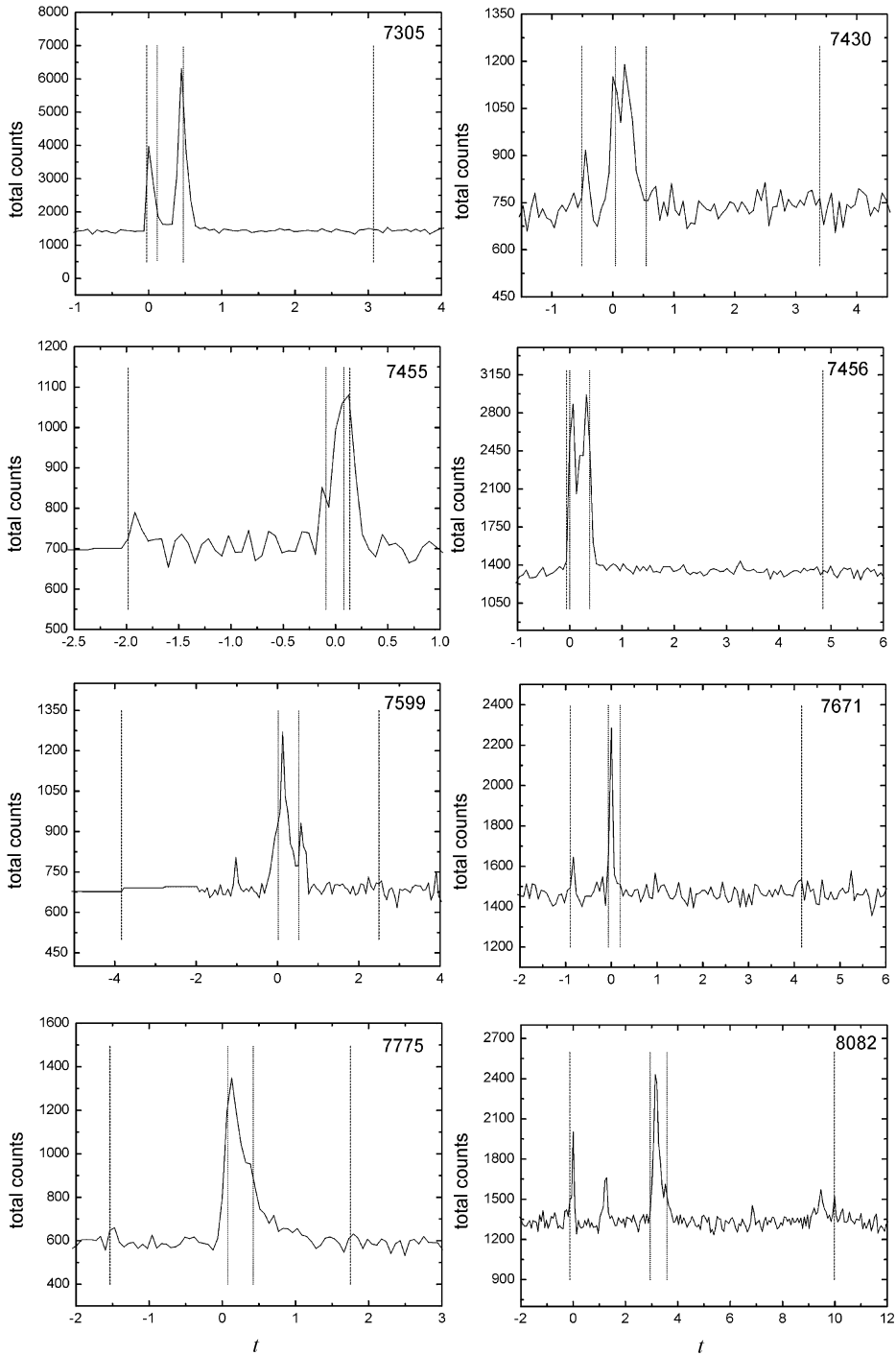


Fig. 7 Continued.

contribute much less. We know that short and long bursts have different hardness ratios (see, e.g., Qin et al. 2000) and that the hardness ratio plays an important role in the classification of GRBs. To find a better way to classify the four bursts, we calculate the average hardness ratio of all the long and short bursts (classified according to  $T_{90}$ ) and get  $\overline{\log \text{HR}} = 0.420 \pm 0.254$  and  $\overline{\log \text{HR}} = 0.718 \pm 0.285$ , respectively. Then we calculate the hardness ratio of 1953, 2988, 7455, and 8082 and obtain  $\log \text{HR} = 0.651, 0.704, 0.699, 0.745$ , respectively. We find that the hardness ratios of these bursts are more close to that of short bursts. Hence it is better to classify these four bursts into short ones.

In these two cases, a common characteristic is that the ratios of  $T_{50}$  to  $T_{90}$  of most of these sources are less than 0.2, while for typical long and short GRBs these ratios are more than 0.4. This indicates that the emission within  $T_{50}$  dominates the total emission. It is believed that short and long bursts originate from distinct progenitors: short bursts are produced by the merger of compact objects, while the core collapse of massive stars would give rise to long bursts (Ghirlanda et al. 2003). Different physical mechanisms of short and long bursts probably have a great effect on the main pulses. From the light curves of these sources, we find that the characteristic of the main pulses of them are similar to that of short bursts. So it is possible that these bursts are produced by the same physical mechanism as short bursts. For this sort of bursts  $T_{50}$  should play an important role in classifying GRBs.

**Acknowledgements** This work is supported by the Special Funds for Major State Basic Research Projects and the National Natural Science Foundation of China (No.10273019).

## References

- Barat C., Hayles R. I., Hurley K. et al., 1984, *ApJ*, 285, 791  
 Belli B. M., 1993, *A&AS*, 97, 63  
 Belli B. M., 1999, *A&AS*, 138, 415  
 Dezalay J. P., Aheia J. L., Basat C. et al., 1992, In: W. S. Paciesas, G. J. Fishman, eds., *Proc. Huntsville Gamma-Ray Burst Workshop*, New York: AIP, p.304  
 Dezalay J. P., Aheia J. L., Basat C. et al., 1997, *ApJ*, 490, L17  
 Fishman G. J., 1999, *A&AS*, 138, 395  
 Fishman G. J., Meegan C. A., Wilson R. B. et al., 1994, *ApJS*, 92, 229  
 Ghirlanda G., Ghisellini G., Celotti A., 2003, *A&A*, submitted, astro-ph/0310861  
 Golenetskii S. V., Mazets E. P., Aptekan R. L. et al., 1983, *Nature*, 306, 451  
 Klebesadel R., Strong I., Olson R., 1973, *ApJ*, 182, L85  
 Kouveliotou C., Meegan C. A., Fishman G. J. et al., 1993, *ApJ*, 413, L101  
 Mallozzi R. S., Paciesas W. S., Pendleton G. N. et al., 1995, *ApJ*, 454, 597  
 Meegan C. A., 1994, *The Second BATSE Burst Catalog*, available electronically from the Compton Observatory Science Support Center  
 Meegan C. A., Paciesas W. S., Pendleton G. N. et al., 1998, In: C. A. Meegan, R. D. Preece, T. M. Koshut, eds., *Gamma-ray Bursts: 4th Huntsville Symp.*, AIP Conf. Proc., 428, p.3  
 Meegan C. A., Pendleton G. N., Briggs M. S. et al., 1996, *ApJS*, 106, 65  
 Paciesas W. S., Meegan C. A., Briggs M. S. et al., 1999, *ApJS*, 122, 465  
 Qin Y. P., Xie G. Z., Xue S. J. et al., 2000, *PASJ*, 52, 759  
 Paciesas W. S., Meegan C. A., Pendleton G. N. et al., 1999, *ApJS*, 122, 465